The EMBO Journal vol.4 no.8 pp.2113–2118, 1985

Three-dimensional structure of the complex of actin and DNase I at 4.5 Å resolution

Wolfgang Kabsch, Hans Georg Mannherz[1] and Dietrich Suck[2]

Max-Planck-Institut für Medizinische Forschung, Jahnstrasse 29, D-6900 Heidelberg, [1]Institut für Anatomie und Zellbiologie der Universität, Robert-Koch-Strasse 6, D-3550 Marburg, and [2]European Molecular Biology Laboratory, Postfach 102209, D-6900 Heidelberg, FRG

Communicated by K.C.Holmes

The shape of an actin subunit has been derived from an improved 6 Å map of the complex of rabbit skeletal muscle actin and bovine pancreatic DNase I obtained by X-ray crystallographic methods. The three-dimensional structure of DNase I determined independently at 2.5 Å resolution was compared with the DNase I electron density in the actin:DNase map. The two structures are very similar at 6 Å resolution thus leading to an unambigous identification of actin as well as DNase I electron density. Furthermore the correct hand of the actin structure is determined from the DNase I atomic structure. The resolution of the actin structure was extended to 4.5 Å by using a single heavy-atom derivative and the knowledge of the atomic coordinates of DNase I. The dimensions of an actin subunit are 67 Å x 40 Å x 37 Å. It consists of a small and a large domain, the small domain containing the N terminus. Actin is an α,β-protein with a β-pleated sheet in each domain. These sheets are surrounded by several α-helices, comprising at least 40% of the structure. The phosphate peak of the adenine nucleotide is located between the two domains. The complex of actin and DNase I as found in solution (i.e., the actin:DNase I contacts which do not depend on crystal packing) was deduced from a comparison of monoclinic with orthorhombic crystals. Residues 44–46, 51, 52, 60–62 of DNase I are close to a loop region in the small domain of actin. At a distance of ~15 Å there is a second contact in the large domain in which Glu13 of DNase I is involved. A possible binding region for myosin is discussed.

Key words: actin/DNase I/X-ray structure

Introduction

F-actin together with the regulatory proteins tropomyosin and troponin constitutes the thin filament in muscle. The F-actin filament can be described as a single-stranded left-hand helix of 13 monomers arranged in six turns repeating in 355 Å. F-actin consists of a single polypeptide chain of 375 amino acid residues, a bound nucleotide (ADP) and a divalent cation (Ca^{2+} or Mg^{2+}). In the absence of salt it can exist as a monomer, G-actin. As judged from the c.d. spectra both actin forms appear to have the same secondary structure. In non-muscle cells, regulation of actin polymerization (for review, see Korn, 1982) serves to control shape, internal organization and movement. Actin interacts with many proteins. The 1:1 complex with DNase I is strong enough to depolymerise F-actin (Lazarides and Lindberg, 1974). This complex can be crystallized in at least three different symmetry groups. Here we compare the monoclinic (form II) with an orthorhombic (form III) crystal form and identify the shape of the solution complex of actin and DNase I. Recently, the structure of DNase I has been determined to atomic resolution (Suck *et al.*, 1984). We exploit this new information to advance the resolution of the actin-DNase I structure to 4.5 Å. Eventually it should prove possible to explain results obtained from chemical cross-linking (Elzinga and Phelan, 1984; Sutoh, 1982; Mornet *et al.*, 1981), reactivity studies of lysine residues (Szilagyi and Lu, 1982; Lu and Szilagyi, 1981; Hitchcock-De Gregori *et al.*, 1982) and fluorescence energy transfer measurements (Miki and Wahl, 1984; Taylor *et al.*, 1981) in terms of the 3-dimensional structure of the actin monomer and thereby arrive at a detailed description of the thin filament assembly and its interaction with myosin.

Results

Improved actin-DNase I electron density map

A new Pb heavy-atom derivative for orthorhombic crystals of the actin:DNase I complex was obtained by co-crystallization as described in Materials and methods. The high quality of this new heavy-atom derivative improved the mean figure of merit from 72% to 80% for all 2117 reflections to 6 Å resolution. An electron-density map of the actin:DNase I complex at 6 Å resolution was calculated by Fourier synthesis using the 'best' protein structure factors (Blow and Crick, 1959) derived from the old derivatives and from the new Pb heavy-atom derivative. All derivatives and heavy-atom parameters used are shown in Tables I and II. A contour model was drawn for a whole unit cell in sections of constant y at intervals of $y/28$. When compared with our original map (Suck *et al.*, 1981) only minor differences were found.

Identification of actin and DNase I in the electron density map

The independent determination of the DNase I structure (Suck *et al.*, 1984) now offer the opportunity to check and improve our original assignment of DNase I density in the orthorhombic map of the actin:DNase I complex. Furthermore it was expected to be able to resolve the exact boundary between actin and DNase I density in the complex.

Following the computational procedure described in Materials and methods a selected DNase I molecule (molecule 1 in Table III) was extracted from the 6 Å actin:DNase I electron

Table I. Heavy atom derivatives

Derivative	Crystal form	Phasing power (F_H/E)	R_C[a] (%)	Resolution (Å)
CH_3HgOAc	II	1.50	53.7	4.5
CH_3HgOAc	III	1.68	51.5	4.5
cis-$PtCl_2(NH_3)_2$	III	1.17	67.8	6.0
$NaReO_4$	III	1.09	67.1	6.0
$Pb(NO_3)_2$	III	2.95	33.8	6.0

[a]R_C Cullis R-factor for centric reflections.

Table II. Heavy atom parameters[a]

Derivative	Crystal form	A	B	x	y	z
CH_3HgOAc	II	0.75	2.3	0.2436	−0.2211[b]	0.2356
		0.75	2.3	0.7436	0.2372	0.2356
CH_3HgOAc	III	1.51	13.0	0.8035	0.9512	0.5666
cis-$PtCl_2(NH_3)_2$	III	0.46	15.0	0.6411	0.6907	0.5004
		1.27	20.0	0.6357	0.2394	0.6766
		1.30	18.6	0.8878	0.6134	0.6689
		0.32	17.1	0.9036	0.3713	0.6238
		0.43	20.9	0.6890	0.7986	0.7986
		0.31	26.7	0.7323	0.0978	0.9511
		0.96	23.0	0.7690	0.8249	0.9295
		0.37	15.0	0.8007	0.6458	0.9794
		0.56	23.4	0.7912	0.0228	0.9421
$NaReO_4$	III	1.06	12.4	0.8049	0.5584	0.7806
$Pb(NO_3)_2$	III	1.52	22.2	0.8141	0.4049	0.8686
		1.10	21.5	0.8476	0.3380	0.8790
		0.42	15.9	0.8436	0.3668	0.7142
		0.48	15.0	0.7740	0.4196	0.8259
		0.64	15.0	0.8059	0.3609	0.8460

[a]Each heavy atom contributes $A \cdot \exp(-B \cdot S^2) \cdot \exp 2\pi i(hx+ky+lz)$ to the structure factor F_{hkl}, and $S=2 \sin \theta/\lambda$.
[b]Arbitrary in monoclinic space group.

Table III. DNase I molecules in contact with actin[a] (orthorhombic crystals)

DNase I molecule number	Fractional coordinates of center of mass of DNase I molecule			Crystallographic symmetry transformation			Distance of DNase I to actin (Å)
	x	y	z				
1	0.60	0.55	0.36	x	y	z	40.5
2	0.60	1.55	0.36	x	$1+y$	z	47.2
3[b]	0.90	0.45	0.86	$1.5-x$	$1-y$	$0.5+z$	46.9
4	0.90	1.45	0.86	$1.5-x$	$2-y$	$0.5+z$	47.0

[a]Actin molecule with center of mass at fractional coordinates 0.68, 0.95, 0.65 is used as reference.
[b]DNase I molecule 3 together with the reference actin forms the solution complex since only this combination occurs also in the monoclinic crystals.

density map. The boundary of this DNase I density was chosen according to our original assignment (Suck *et al.*, 1981) and was expected to be somewhat in error, especially at the interface region to another DNase I molecule and to actin. The same procedure was repeated for a selected DNase I molecule in the map obtained by independent X-ray analysis of crystals (Suck *et al.*, 1984) containing only DNase I without actin. The two DNase I molecules were compared at all possible relative orientations (steps of 5°) using the fast rotation function method (Crowther, 1972; Tanaka, 1977). As a result a unique best rotation was found. To find the translation between the two selected DNase I molecules, their centres were superimposed and subsequently refined using the fast translation function (Crowther and Blow, 1967). For a visual control the electron density of DNase I determined independently at 2.5 Å resolution was transformed to the same orientation as the DNase I density in the actin:DNase I map and reduced to 6 Å resolution. It was found that our original boundary between actin and DNase I was quite accurate but the interface between two symmetry-related DNase I molecules was somewhat in error. Therefore the procedure described above was repeated with the corrected DNase I boundary. The result is shown in Figure 1. Except for the carbohydrate attached to Asn18, the two DNase I molecules look very similar at 6 Å resolution. In addition, it is obvious from this comparison that the correct hand – and not its mirror image – was chosen in the improved and original (Suck *et al.*, 1981) actin:DNase I map.

Applying the transformation determined above to the Pb sites in the DNase I crystals (Table II in Suck *et al.*, 1984) we find three corresponding substitution sites of our new Pb derivative for actin:DNase I crystals. Indeed, Pb sites 3, 5 and 6 in the DNase I crystals can be superimposed (Kabsch, 1978) with the first three Pb sites in the actin:DNase I crystals. The root-mean-square error is 0.7 Å.

Comparison of cytoplasmic and skeletal muscle actin structure

Crystals of a cytoplasmic (porcine liver) actin in complex with DNase I were also obtained (Mannherz *et al.*, 1985). These crystals were found to be isomorphous to the orthorhombic type III crystals containing rabbit skeletal muscle actin although the two actins differ in 25 amino acids. A native and a methylmercury acetate heavy-atom derivative data set were collected on a diffractometer to a resolution of 7 and 6 Å, respectively. Instead of the single mercury substitution site as found in the rabbit skeletal muscle actin structure (Table II) several sites of low significance appeared in the difference Fourier map. A most plausible explanation for the missing dominant substitution site in cytoplasmic actin is the change of Cys to Val at residue 10 in the amino acid sequence (Elzinga *et al.*, 1973; Korn, 1982). The free sulfhydryl residue at position 17 in the cytoplasmic actin sequence does not seem to react with methylmercury acetate in the crystal. The mercury substitution site near Cys10 in rabbit skeletal muscle is marked 'M' in Figure 2. It is located halfway between a helix and the β-sheet in the small domain. Although it remains unclear to which of the two objects Cys10 belongs, we conclude from the details of the map that the N terminus of actin is located in the small domain.

Structure of actin at 4.5 Å resolution

Knowledge of the atomic coordinates of DNase I and the orientation of the molecule in the actin:DNase I crystals was combined with the single isomorphous data of the mercury derivative to 4.5 Å resolution and all other derivative information obtained so far to 6 Å resolution (Sim, 1959; Hendrickson and Lattman, 1970). An electron density map of a portion of the unit cell containing one actin molecule was drawn at a scale of 3 mm/Å. In agreement with earlier work (Suck *et al.*, 1981) actin consists of a small and a large domain, representing 40% and 60% of the density, respectively. Many rod-like features appeared in both domains of actin. Although we cannot identify side chains at this resolution, pitch and diameter of ideal helices could be fitted interactively on our display. At least 40% of the actin structure appear to be α-helical. Furthermore, each domain contains a β-sheet surrounded by several helices. The highest density representing the phosphate peak of the bound adenine nucleotide is found between the two actin domains at the same place as in the 6 Å map. This place is marked 'P' in Figure 2. Figure 3 shows a portion of the map at 4.5 Å resolution containing the β-sheet and surrounding helices in the small domain of actin.

Solution complex of actin and DNase I

In the orthorhombic form III crystals each actin monomer is found in contact with four DNase I molecules (Table III). One of these possible combinations should also occur in the monoclinic form II crystals since there exists a unique 1:1 complex of actin:DNase I in solution from which both crystal forms were obtained under nearly identical conditions. We compare now

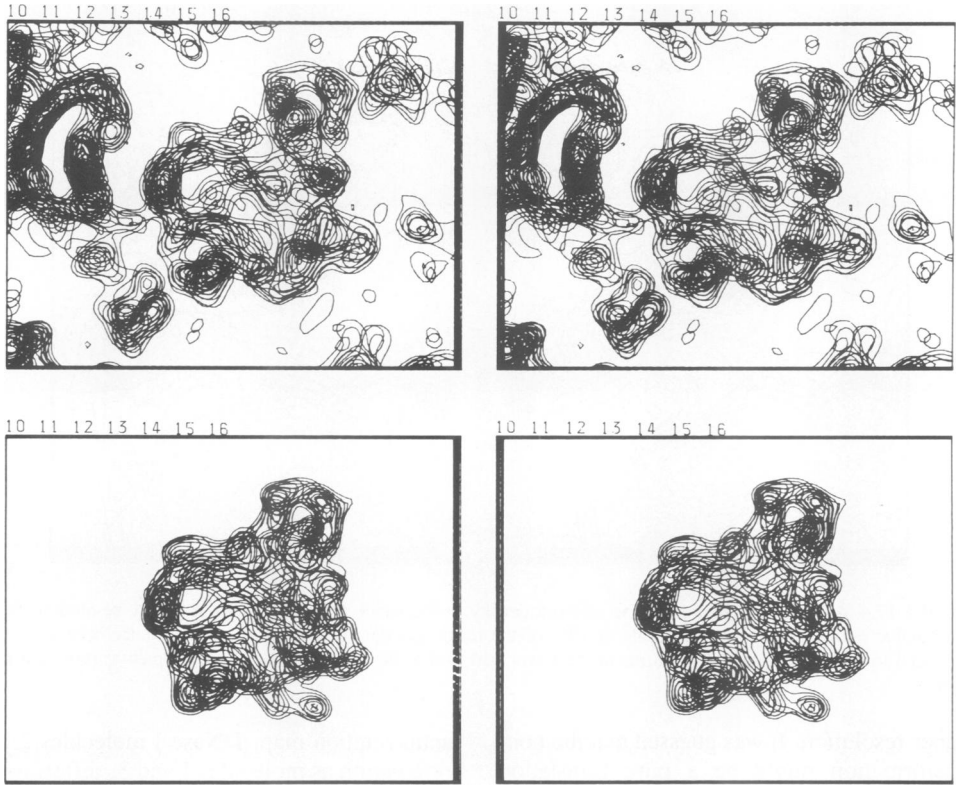

Fig. 1. Comparison at 6 Å resolution of DNase I electron densities obtained from independent crystal structure analyses. **Top:** stereoscopic view of a portion of the electron density map of the orthorhombic unit cell containing rabbit skeletal muscle actin:DNase I complex. Sections 10/24 to 16/24 perpendicular to the *b*-axis contoured at intervals of 10% of the maximum density are shown. The distance between sections is 2.35 Å. **Bottom:** stereoscopic view of the electron density of DNase I calculated from the atomic positions. The structure of DNase I was reduced to 6 Å resolution and oriented to fit the DNase I molecule shown above. The two DNase I molecules are very similar at this resolution. The ill-defined carbohydrate density was omitted in the comparison.

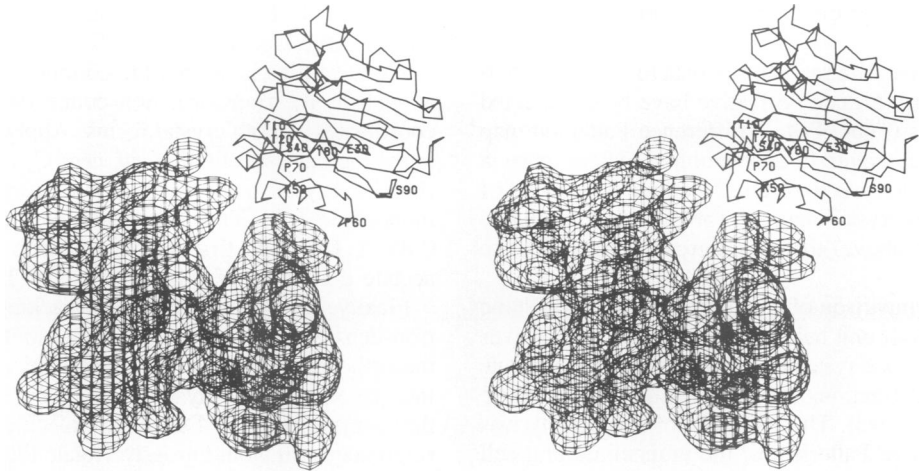

Fig. 2. Stereoscopic view of the solution complex of actin and DNase I. The electron density of the actin monomer was extracted from the improved orthorhombic actin:DNase I map at 6 Å resolution and contoured at 10% of the maximum density. The dimensions of actin are 67 Å x 40 Å x 37 Å. Actin consists of a large (~60% of the total mass) and a small domain with a pronounced cleft in between. The highest electron density peak is found in the cleft probably representing the bound nucleotide and marked as 'P'. 'M' points to the mercury-binding site at Cys10 in rabbit skeletal muscle actin. DNase I is represented as a polygon connection adjacent C_α-positions. The identity of some residues near the contact region to actin is specified. DNase I residues 44–46, 51, 52, 60–62 are close to a loop region in the small domain of actin. At a distance of ~15 Å from the major contact region Glu13 of DNase I is involved in a second contact, probably a salt bridge, to the large domain of actin.

these two crystal forms and identify the combination of actin and DNase I density common to both crystal forms.

A summary of the native data set of the monoclinic form II crystals is shown in Table IV. Up to 6 Å resolution, intensities of reflections with indices $h+k$=even are much stronger than those with $h+k$=odd. Although form II crystals belong to space group $P2_1$ with two molecules in the asymmetric unit (Suck *et al.*, 1981), at low resolution these crystals can be described by C2 symmetry with one molecule in the asymmetric unit. The observed asymmetry of the reflection intensities gradually

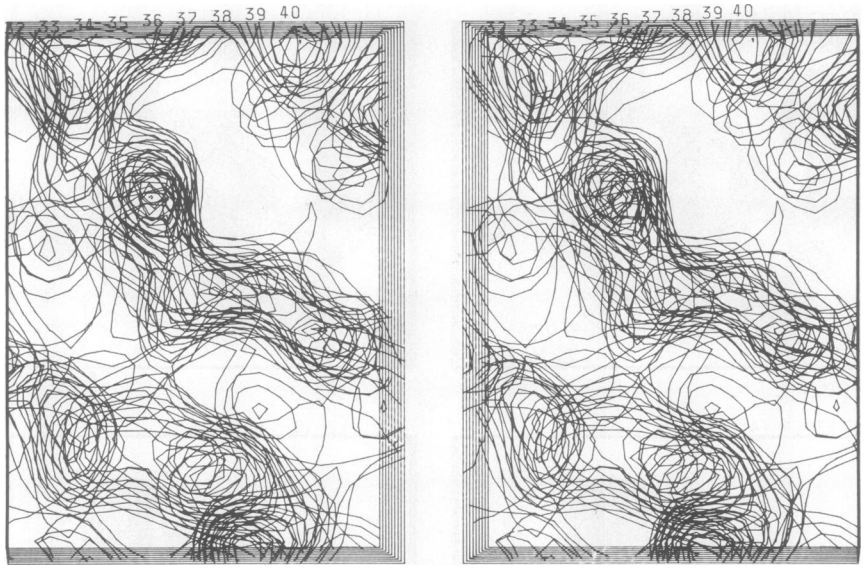

Fig. 3. Stereoscopic view of a 17.4 Å x 23.9 Å portion of the electron density in the small domain of actin at 4.5 Å resolution. Sections 32/36 to 40/36 perpendicular to the orthorhombic *b*-axis contoured at intervals of 10% of the maximum density are shown. The distance between sections is 1.57 Å. Individual β-strands are parallel to the drawing plane. Features at the lower part and at the upper right part of the picture represent portions of helices packing on both sides of the β-sheet.

regresses towards higher resolution. It was guessed that the non-crystallographic transformation might be a pure translation deviating slightly from exact C2 symmetry. Therefore, a native Patterson map including all data to 3 Å resolution was calculated. Indeed, besides the origin peak, the map contains a sharp maximum at $u=0.5$ $v=0.4583$ $w=0$. The peak height is 30% of the origin peak (reflection 0, 0, 0 omitted). We conclude that the non-crystallographic symmetry essentially consists of a pure translation $t=0.5a + 0.4583b$. Consistent with that, no additional peaks besides the crystallographic ones were found in the self-rotation map.

In addition to the native data set intensity data to ~5 Å resolution of a methylmercury acetate derivative have been collected for the form II crystals (Table IV). A difference Patterson map was calculated, and subsequently deconvoluted. There exists a single mercury substitution site for each of the four actin:DNase I molecules in the form II crystal unit cell (Table II). It seems likely (as has been discussed above) that this mercury site is close to Cys10 in actin.

For a quantitative comparison of both crystal forms we assume that *a* and *b* axes of both unit cells coincide with *X* and *Y* axes of an orthonormal reference system. We chose the actin molecule with center of mass at fractional coordinates 0.68, 0.95, 0.65 in the orthorhombic unit cell. The Patterson of this density was compared with the native Patterson of the monoclinic unit cell in all possible orientations. Three independent maxima of the overlap integral were obtained, the values of the second and third peak being 99% and 86% of the first and largest peak (step size 1° around the peaks). It was found impossible to pack the actin monomer oriented according to the second peak into the monoclinic crystal.

The same procedure was repeated for DNase I molecules 1 and 3 in contact with the reference actin in the orthorhombic cell (Table III). None of the major peaks of these maps were found close to the second and third peak in the actin rotation map, supporting our suspicion that these peaks are artifacts. Fortunately, for DNase I molecule 3 the strongest peak in the rotation map occurred only 3° off the position of the strongest peak in the actin rotation map. DNase I molecules 2 and 4 are in the same orientation as molecules 1 and 3, differing only by a translation. Hence their rotation maps would be identical. As a result we can exclude DNase I molecules 1 and 2. To find out whether DNase I molecules 3 or 4 form the correct actin:DNase I complex we tried both possibilities. In each case we applied the rotation determined above to the densities and searched their origin in the monoclinic cell using the fast translation function method (Crowther and Blow, 1967). Only for DNase I molecule 3, together with the reference actin, a unique peak appeared, the second largest peak was at 80% of the maximum.

We have thus identified the common actin:DNase I complex as well as the transformation connecting equivalent fractional coordinates of both crystal forms. Applying this transformation to the mercury substitution site near Cys10 in actin in the orthorhombic crystal form we find its corresponding position in the monoclinic cell. This calculated position is at a distance of 0.85 Å from the first substitution site of the methylmercury acetate derivative of form II crystals (Table II).

Finally, for a visual control of packing consistency, an electron density map of the monoclinic unit cell was drawn using the orthorhombic density. Despite the short *b* axis (42 Å) no interpenetrating density was found. Furthermore we noted that the combination of DNase I molecule 4 together with the reference actin would grossly violate these packing constraints.

We conclude that the combination of the reference actin and DNase I molecule 3 is the unique invariant which does not depend on specific crystal packing. We expect that this complex also occurs in solution. Figure 2 shows that the main contact occurs at the small domain of actin and involves residues 44–46, 51, 52, 60–62 of DNase I. There is a minor contact region, probably a salt bridge, between the large domain of actin and Glu13 of DNase I.

Discussion

From the results obtained so far the following picture emerges: an actin subunit has dimensions 67 Å x 40 Å x 37 Å. It consists of a large and a small domain comprising ~60% and 40%

Table IV. Oscillation data collection (monoclinic crystals)

(a) Intensity statistics of native data set (combined partial data sets 1 and 2

Resolution (Å)	Reflection type	Number[a] observed reflections	Completeness of data (%)	Average reflection intensity
∞ – 6	$h+k$=even	1556	86	7.4
	$h+k$=odd	1114	61	1.9
6 – 4	$h+k$=even	3482	81	5.9
	$h+k$=odd	2736	63	3.7
4 – 3	$h+k$=even	3822	46	3.5
	$h+k$=odd	3404	40	3.2

(b) Partial native data set 1 (60 film packs)

Resolution (Å)	Number[a] observed reflections	Completeness of data (%)	R_{sym}[b] (%)	R_{scale}[c] (%)	R_{comb}[d] (%)
∞ – 6	1978	54	2.8	5.3	7.8
6 – 4	4702	55	3.4	6.3	9.1
4 – 3	5597	33	5.9	9.1	14.0

(c) Partial native data set 2 (41 film packs)

Resolution (Å)	Number[a] observed reflections	Completeness of data (%)	R_{sym}[b] (%)	R_{scale}[c] (%)	R_{comb}[d] (%)
∞ – 6	2091	58	4.3	6.1	12.8
6 – 4	4375	51	3.9	8.7	17.1
4 – 3	3738	22	9.5	11.1	23.3

(d) CH_3HgOAc derivative data set (36 film packs)

Resolution (Å)	Number[a] observed reflections	Completeness of data (%)	R_{sym}[b] (%)	R_{scale}[c] (%)	R_{comb}[d] (%)
∞ – 6	2206	61	3.4	6.5	10.8
6 – 4	4017	47	5.9	10.1	14.9

[a]Number of observed reflections includes only independent reflections with signal-to-noise ratio >3.
[b]Intensities I_{hi} of fully recorded symmetry-related reflections on the same film are compared with their mean intensity I_h.
[c]Intensities I_{hi} of all fully recorded symmetry-related reflections on any film are compared with their mean intensity I_h.
[d]Combined intensities I_{hi} of partially recorded reflections on any film are compared with their 'true' intensity I_h. Reliability factors are defined here as $R = \sum_{hi} |I_{hi} - I_h| / \sum_{hi} I_{hi}$

of the total mass, respectively. The high-affinity nucleotide-binding site is located in between the two domains. Actin is an α,β-protein with a β-sheet in each domain. These sheets are surrounded by several α-helices comprising at least 40% of the structure.

In solution, DNase I binds to both the large and the small domain of actin. In the contact with the large domain only Glu13 of DNase I is involved. It probably forms a salt bridge. The main interaction occurs at the small domain of actin and includes residues 44 – 46, 51, 52, 60 – 62 of DNase I. It is conceivable that complex formation with DNase I inhibits relative movements of the actin domains.

The rapid denaturation of nucleotide-free actin demonstrates the importance of ATP/ADP for the structural stability of the protein. The strategic position of the adenine nucleotide in between the two domains might be important in controlling the relative orientation of the two folding units. In agreement with this hypothesis, by fixing the relative orientation of the actin domains through forming the complex with DNase I it is observed that the nucleotide exchange rate is markedly reduced (Mannherz *et al.*, 1980).

Our crystallographic results indicate that the mercury substitution site near Cys10 is located halfway between a helix and the β-sheet in the small domain. Hence we cannot yet decide whether Cys10 is in a helix or in a β-strand. However, as judged from the electron density helix, either assumption would assign the N terminus in the small domain.

In solution, DNase I mainly binds at a loop region in the small domain of actin. There is evidence from reactivity studies of Lys residues (Ng and Burtnick, 1982) and chemical cross-linking experiments (Sutoh, 1984) that Lys61 or Lys68 must be close to this loop in the small domain of actin. Knowing that Cys10 and Lys61 or Lys68 are both located in the small domain of actin, it is tempting to speculate that the amino acid sequence of actin consists of two portions each representing a folding domain. From the observed domain size we would expect residues 1 to ~150 to form the small domain. This hypothesis is supported by the recent finding of a hybrid protein containing the N-terminal portion of actin (residues 1 to ~140) and a tyrosine-specific protein kinase (Naharro *et al.*, 1983).

Recently it has been shown that the N-terminal (residues 1 – 11) and C-terminal segments (residues 358 – 372) of actin participate in binding depactin, a small actin-depolymerizing protein of mol.wt 17 000 (Sutoh and Mabuchi, 1984). The depactin and DNase I binding sites are known to be spatially distinct since the actin:depactin complex can bind to a DNase I-Sepharose column (Mabuchi, 1983). Furthermore, the binding site of depactin overlaps with that of myosin on actin (Sutoh, 1983). Therefore, it is conceivable that the myosin binding region covers adjacent parts of the actin domains opposite to the DNase I binding sites (Figure 2).

Materials and methods

Purification and crystallisation

Protein preparations and crystallisations were done as described (Suck *et al.*, 1981). Rabbit skeletal muscle actin was prepared from dry acetone powder including two cycles of polymerization and depolymerization. DP-grade bovine pancreatic DNase I was purchased from Worthington and purified by chromatography on hydroxyapatite. Actin:DNase I complex was formed by mixing purified actin and DNase I at equimolar concentrations for 1 h at room temperature. Prior to crystallisation the complex solution was subjected to a mild tryptic treatment which removes three amino acids – including Cys374 – at the C terminus of actin. Monoclinic (form II) and orthorhombic (form III) crystals of actin:DNase I were obtained at pH 6.6 by adding 8 – 10% polyethyleneglycol 6000 as precipitating agent. The buffer solution contained 50 mM imidazole, 0.1 mM $CaCl_2$, 1 mM NaN_3 and 2 mM MgATP. The monoclinic crystals belong to space group $P2_1$ with unit cell parameters a=153.0 Å b=42.2 Å c=122.2 Å β=108.2° and contain two actin:DNase I molecules in the asymmetric unit. The orthorhombic crystals were initially obtained in a batch of monoclinic crystals and later reproducibly grown by seeding with small orthorhombic crystals. These crystals belong to space group $P2_12_12_1$ with a=133.0 Å b=56.4 Å c=110.0 Å and contain one actin:DNase I molecule in the asymmetric unit. In view of the instability of ATP and the long duration of crystal growth it is likely that the actin bound nucleotide is ADP. Furthermore, in solution actin-bound [^{3}H]ATP is hydrolyzed into [^{3}H]ADP within 24 h when in complex with DNase I. Similarly the analysis of actin-bound nucleotide after dissolving type III crystals indicates that the nucleotide is ADP. The assay used is based on the optically linked ADP-regenerating system as described in Mannherz *et al.* (1974).

Heavy atom derivatives and data collection

Isomorphous heavy atom derivatives (Hg, Pt and Re) were prepared by soaking native type III crystals as described (Suck *et al.*, 1981). A new derivative was obtained by adding 10-fold molar excess of $Pb(NO_3)_2$ to DNase I prior to com-

plex formation with actin. During the trypsin treatment of the complex and subsequent crystallisation the lead nitrate concentration was kept at 0.1 mM. X-ray reflections from orthorhombic crystals were measured on a Syntex $P2_1$-4-circle diffractometer as described (Suck *et al.*, 1981). Data to 6 Å were collected for the Pt, Re and Pb derivatives, 4.5 Å data sets for native and Hg derivative. The heavy atom positions of the new Pb derivative were derived from a difference Fourier. The parameters of all derivatives were refined simultaneously using a procedure similar to that of Dickerson *et al.* (1968). The final result is given in Table II. The quality and phasing power of these derivatives is displayed in Table I. The figure of merit for all reflections to 6 Å is 0.80.

For the monoclinic type II crystal form a heavy atom derivative was obtained by soaking with a 1 mM methylmercury acetate solution for 1.5 h. Native data to 3 Å and derivative data to 5 Å were collected on films using a rotation camera (Arndt *et al.*, 1973) aligned to an Elliott GX6 rotating anode. The films were digitized using a rotating-drum scanner (Optronics International Inc., MA) and evaluated subsequently by an oscillation data processing system (Kabsch, 1977). The native data set was obtained from two partial data sets recorded on 60 and 41 oscillation photographs (Table IV). To cover the 'blind' region, crystals were mounted with either their *b* or *c** axis along the oscillation axis. At low resolution the average diffraction intensity is stronger for reflections with even $h+k$ than for odd $h+k$. This is due to the non-crystallographic symmetry of the monoclinic crystals. At low resolution their space group reduces to C2 with one molecule per asymmetric unit.

Rotation and translation search methods

For a quantitative comparison of identical molecules each in a different crystallographic environment we need to determine their relative position and orientation. Usually, the three parameters of the rotation are derived from the position of maximum overlap between the fixed Patterson of the first crystal and the rotated Patterson of the second crystal. To accelerate computation, the Patterson densities are expanded in terms of spherical harmonics and Bessel functions (Crowther, 1972; Tanaka, 1977). Results are much clearer if intermolecular difference vectors can be eliminated from the Patterson function. This was achieved by the following procedures: the electron density of a full unit cell of the actin:DNase I complex was displayed successively in 28 sections at constant *y* on an interactive color graphics system designed in our laboratory (W.Gebhard and W.Kabsch, unpublished results). For a selected molecule (either actin or DNase I) its boundary on each section was outlined interactively using an *xy*-tablet as a graphics input device. All density outside the selected molecule was then discarded. The remaining density was transferred into a somewhat larger fictive triclinic unit cell. The Patterson function calculated now represents only intramolecular difference vectors. To determine the rotation we vary its three angular parameters in steps of 5° and calculate, at each position, how well the Pattersons overlap within a sphere of 18 Å around the origin. Near a peak, angular step size was decreased to 1°.

To position the oriented molecule we expressed its Patterson in the relevant crystallographic environment as a function of the three unknown translation parameters. If the molecule is placed correctly the overlap between its calculated and observed Patterson is a maximum. Again, the overlap function can be expressed conveniently in the form of a Fourier series (Crowther and Blow, 1967).

Acknowledgements

We thank Mrs. H.Pfrang for excellent technical assistance and Dr. K.C.Holmes for his interest and helpful discussions.

References

Arndt,U.W., Champness,J.N., Phizackerley,R.P. and Wonacott,A.J. (1973) *J. Appl. Crystallogr.*, **6**, 457-463.
Blow,D.M. and Crick,F.H.C. (1959) *Acta Crystallogr.*, **12**, 794-802.
Crowther,R.A. (1972) in Rossmann,M.G. (ed.), *The Molecular Replacement Method*, Gordon & Breach, NY, USA, pp. 173-183.
Crowther,R.A. and Blow,D.M. (1967) Acta Crystallogr., **23**, 544-548.
Dickerson,R.E., Weinzierl,J.E. and Palmer,R.A. (1968) *Acta Crystallogr.*, **B24**, 997-1003.
Elzinga,M. and Phelan,J.J. (1984) *Proc. Natl. Acad. Sci. USA*, **81**, 6599-6602.
Elzinga,M., Collins,J.H., Kuehl,W.M. and Adelstein,R.S. (1973) *Proc. Natl. Acad. Sci. USA*, **70**, 2687-2691.
Hendrickson,W.A. and Lattman,E.E. (1970) *Acta Crystallogr.*, **B26**, 136-143.
Hitchcock-De Gregori,S., Mandala,S. and Sachs,G.A. (1982) *J. Biol. Chem.*, **257**, 12573-12580.
Kabsch,W. (1977) *J. Appl. Crystallogr.*, **10**, 426-429.
Kabsch,W. (1978) *Acta Crystallogr.*, **A34**, 827-828.
Korn,E.D. (1982) *Physiol. Rev.*, **62**, 672-737.
Lazarides,E. and Lindberg,U. (1974) *Proc. Natl. Acad. Sci. USA*, **71**, 4742-4746.
Lu,R.C. and Szilagyi,L. (1981) *Biochemistry (Wash.)*, **20**, 5914-5919.
Mabuchi,I. (1983) *J. Cell Biol.*, **97**, 1612-1621.
Mannherz,H.G., Schenck,H. and Goody,R.S. (1974) *Eur. J. Biochem.*, **48**, 287-295.
Mannherz,H.G., Goody,R.S., Konrad,M. and Nowak,E. (1980) *Eur.J. Biochem.*, **104**, 367-379.
Mannherz,H.G., Kabsch,W., Suck,D., Friebel,K. and Frimmer,M. (1985) *Biochem. J.*, **225**, 517-522.
Miki,M. and Wahl,P. (1984) *Biochim. Biophys. Acta*, **790**, 275-283.
Mornet,D., Bertrand,R., Pantel,P., Audemard,E. and Kassab,R. (1981) *Nature*, **292**, 301-306.
Naharro,G., Robbins,K.C. and Reddy,E.P. (1983) *Science (Wash.)*, **223**, 63-66.
Ng,J.S.Y. and Burnick,L.D. (1982) *Int. J. Biol. Macromol.*, **4**, 215-218.
Sim,G.A. (1959) *Acta Crystallogr.*, **12**, 813-815.
Suck,D., Kabsch,W. and Mannherz,H.G. (1981) *Proc. Natl. Acad. Sci. USA*, **78**, 4319-4323.
Suck,D., Oefner,C. and Kabsch,W. (1984) *EMBO J.* **3**, 2423-2430.
Sutoh,K. (1982) *Biochemistry (Wash.)*, **21**, 3654-3661.
Sutoh,K. (1983) *Biochemistry (Wash.)*, **22**, 1579-1585.
Sutoh,K. (1984) *Biochemistry (Wash.)*, **23**, 1942-1946.
Sutoh,K. and Mabuchi,I. (1984) *Biochemistry (Wash.)*, **23**, 6757-6761.
Szilagyi,L. and Lu,R.C. (1982) *Biochim. Biophys. Acta*, **709**, 204-211.
Tanaka,N. (1977) *Acta Crystallogr.*, **33**, 191-193.
Taylor,D.L., Reidler,J., Spudich,J.A. and Stryer,L. (1981) *J. Cell Biol.*, **89**, 362-367.

Received on 20 May 1985